

Circularly and elliptically polarized near-field radiation from nanoscale subwavelength apertures

Erdem Ögüt and Kürşat Şendur

Citation: *Appl. Phys. Lett.* **96**, 141104 (2010); doi: 10.1063/1.3371696

View online: <http://dx.doi.org/10.1063/1.3371696>

View Table of Contents: <http://apl.aip.org/resource/1/APPLAB/v96/i14>

Published by the [American Institute of Physics](#).

Additional information on Appl. Phys. Lett.

Journal Homepage: <http://apl.aip.org/>

Journal Information: http://apl.aip.org/about/about_the_journal

Top downloads: http://apl.aip.org/features/most_downloaded

Information for Authors: <http://apl.aip.org/authors>

ADVERTISEMENT



Goodfellow
metals • ceramics • polymers • composites
70,000 products
450 different materials
small quantities fast

www.goodfellowusa.com

Circularly and elliptically polarized near-field radiation from nanoscale subwavelength apertures

Erdem Ögüt and Kürşat Şendur^{a)}

Sabancı University, Orhanlı-Tuzla, 34956 Istanbul, Turkey

(Received 17 December 2009; accepted 28 February 2010; published online 5 April 2010)

With advances in nanotechnology, obtaining circularly and elliptically polarized optical spots beyond the diffraction limit is an emerging need for plasmonic applications. Two techniques are suggested to obtain circularly and elliptically polarized near-field radiation using subwavelength apertures. It is demonstrated that a square aperture can mediate diffraction limited circularly or elliptically polarized radiation into an optical spot with circular or elliptical polarization beyond the diffraction limit. Linearly polarized diffraction limited radiation is converted into a circularly or an elliptically polarized optical spot beyond the diffraction limit by creating asymmetry in the subwavelength aperture. © 2010 American Institute of Physics. [doi:10.1063/1.3371696]

Near-field radiation from subwavelength apertures is a means of obtaining tightly localized optical spots to beat the diffraction limit.¹ Near-field radiation from small circular apertures on perfectly conducting metals has been extensively studied.^{2,3} The decline in transmission intensity with the fourth power of aperture size leads to very low transmission intensity obtained from subwavelength apertures on perfectly conducting metals. Following the groundbreaking work of Ebbesen,⁴ enhancing the transmission intensity from subwavelength apertures using various techniques has attracted much interest.⁴⁻⁹ Although significant literature exists on improving transmission intensity, the polarization aspects of radiation from subwavelength apertures have been largely ignored. In this study, obtaining localized light with various polarizations through nanoscale subwavelength apertures will be addressed.

Polarized electromagnetic radiation has led to interesting technical applications and significant advancements at both optical and microwave frequencies. With advances in nanotechnology, electromagnetic radiation beyond the diffraction limit with a particular polarization is an emerging need for plasmonic applications. Among these, all-optical magnetic recording¹⁰ requires circularly polarized optical spots. It has been demonstrated that the magnetization can be reversed in a reproducible manner using a circularly polarized optical beam without an externally applied magnetic field.¹⁰ To advance the areal density of hard disk drives beyond 1 Tbit/in.², a sub-100 nm circularly polarized optical spot beyond the diffraction limit is required.

Recently, there has been growing interest in obtaining optical spots with various polarizations beyond the diffraction limit. Ohdaira *et al.*¹¹ obtained local circular polarization by superposing two cross propagating evanescent waves. It has been recently demonstrated that the polarization of diffraction limited incident beams can be manipulated using nanoparticle based antenna geometries¹²⁻¹⁵ and nanorod arrays.¹⁶ Elliptically and circularly polarized near-field radiation can also be achieved through subwavelength apertures by utilizing a circular hole surrounded by elliptical gratings¹⁷ and L-shaped hole arrays.¹⁸

In this study, two alternative techniques are investigated to obtain circularly and elliptically polarized near-field radiation from subwavelength apertures. (1) A square aperture can mediate diffraction limited circularly or elliptically polarized radiation into an optical spot with circular or elliptical polarization beyond the diffraction limit. (2) Diffraction limited linear polarization can be converted into a circularly or elliptically polarized optical spot beyond the diffraction limit by creating and carefully adjusting an asymmetry in the aperture dimensions, as well as adjusting the polarization angle of the incident light.

In the first part of this study, a square aperture is investigated to obtain elliptical and circular polarized optical spots. To analyze this problem, a three-dimensional frequency-domain finite element method (FEM) is utilized.^{19,20} The accuracy of the solution technique was previously validated by comparison with other solution techniques.^{19,20} The total electric field $\mathbf{E}^t(\mathbf{r})$ is composed of incident field $\mathbf{E}^i(\mathbf{r})$ and scattered field $\mathbf{E}^s(\mathbf{r})$. In this study, the incident field is a plane wave. To obtain the scattered field $\mathbf{E}^s(\mathbf{r})$ we used an FEM based full-wave solution of Maxwell's equations. To represent the scattering geometries accurately, tetrahedral elements are used to discretize the computational domain. On the tetrahedral elements, edge basis functions and second-order interpolation functions are used. Adaptive mesh refinement is used to improve the coarse solution regions with high field intensities and large field gradients.

Figure 1(a) illustrates a square aperture and a circularly polarized incident beam. In this study, an isolated nanohole on a gold thin-film is used. The computational volume of the

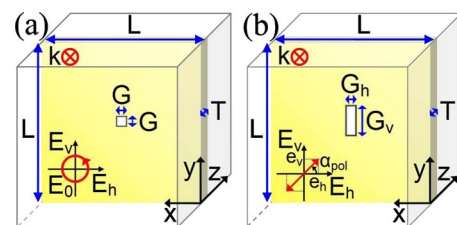


FIG. 1. (Color online) (a) A square aperture illuminated with circular or elliptical polarization. (b) A rectangular aperture illuminated with linear polarization with a polarization angle of α_{pol} .

^{a)}Electronic mail: sendur@sabanciuniv.edu.

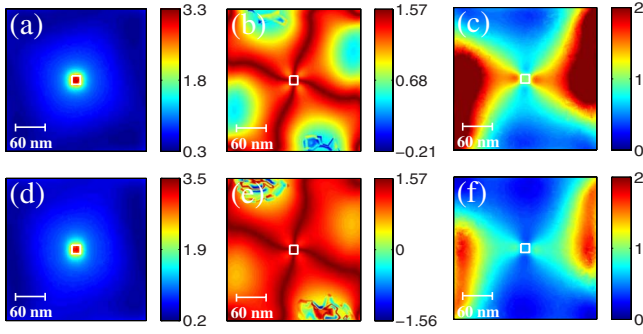


FIG. 2. (Color online) Intensity, phase difference, and intensity ratio distributions for nanoapertures at $z=20$ nm. First and second rows are for circularly and elliptically polarized illuminations, respectively. [(a) and (d)] $|E|^2$, [(b) and (e)] $|\Delta\phi|$, and [(c) and (f)] $|E_y|/|E_x|$. The projection of the aperture boundaries (thin white contour) is also illustrated.

model is illustrated in Fig. 1 by a transparent rectangular box. The metallic thin film is represented by a rectangular box with a hole for the isolated aperture. The transparent rectangular box represents the surrounding vacuum, and has a total thickness of 300 nm along the z -direction. At the outer surfaces of the computational volume in Fig. 1, radiation boundary conditions are applied to ensure that the outgoing electromagnetic field does not reflect back into the computational volume. The edge-length of the square aperture is $G=20$ nm. The length L is selected as 330 nm. In the second part of this study, symmetry condition for the aperture will be relaxed and different aperture dimensions will also be used, as shown in Fig. 1(b). The thickness of the thin film is selected as $T=20$ nm. The operating wavelength is selected as $\lambda=550$ nm, which corresponds to the resonance wavelength of the aperture geometry. The dielectric constants of gold at $\lambda=550$ nm is chosen as $\epsilon_{\text{gold}}=-7.1113+j1.9342$.²¹ A plane wave with an amplitude of 1 V/m is utilized as the incident optical field intensity. This represents an optical field with a uniform intensity over the entire structure.

Figures 2(a) and 2(d) illustrate the intensity distribution for the aperture when it is illuminated with a diffraction limited circularly and elliptically polarized light. The intensity distribution is illustrated at $z=20$ nm. This plane is located at a distance of 10 nm below the bottom surface of the aperture, therefore, it represents a typical intensity distribution on the sample plane.

To obtain circular polarization within the localized optical spot, two requirements need to be met: a phase difference $\Delta\phi=90^\circ$ and a unit amplitude ratio E_y/E_x in the vicinity of the aperture. Due to the symmetry of the geometry $\Delta\phi=90^\circ$ is obtained in the gap region of the aperture as shown in Fig. 2(b). To obtain a circularly polarized optical spot, the

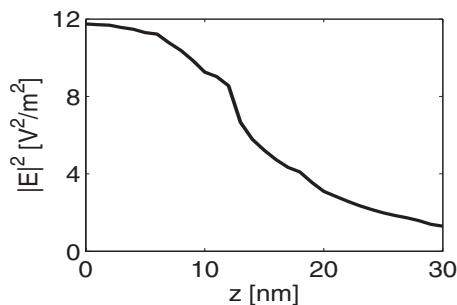


FIG. 3. Intensity distribution as a function of distance from the aperture.

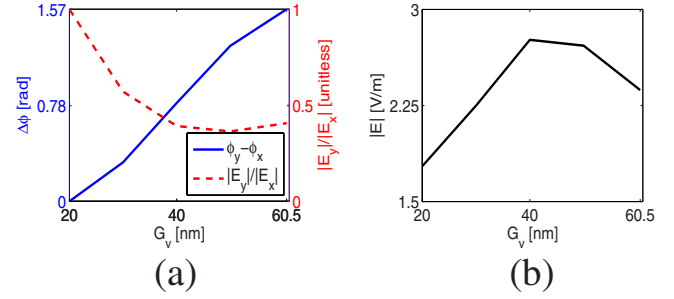


FIG. 4. (Color online) Effect of various G_v values on (a) $|\Delta\phi|$ and $|E_y|/|E_x|$, (b) $|E|^2$ for $G_h=20$ nm, and $T=20$ nm.

90° phase difference requirement needs to be satisfied around the gap region. As shown in Fig. 2(c), the relative amplitude of the horizontal and vertical field is the same within the optical spot due to the symmetry of the geometry. Therefore, the unit amplitude ratio requirement is also satisfied within the optical spot. The results in Figs. 2(a)–2(c) indicate that a circularly polarized optical spot is obtained around the aperture. To obtain elliptical polarization a nonzero phase difference is sufficient. As seen in Fig. 2(e), a nonzero phase difference is obtained around the aperture. The sense of circular and elliptical polarizations is left-handed, since the field propagates in the positive z -direction. Figure 3 illustrates the intensity distribution as a function of distance from the aperture. The results in Fig. 3 suggest that the attenuation length through the nanohole is about 16 nm.

Local surface plasmons (LSP) play an important role in obtaining intense optical spots with circular and elliptical polarization, as shown in Fig. 2. As an example, circularly polarized radiation can be considered. It can be decomposed into a horizontal and vertical component of equal amplitude with a 90° phase difference. Each of these components interacts with the aperture on the gold thin film and excite the LSP. Since the incident beam is composed of horizontal and vertical components with equal amplitude, the LSP in the horizontal and vertical directions also have equal amplitude and a 90° phase difference, which causes the resulting optical spot to be circularly polarized.

In the second part, a rectangular aperture with dimensions G_h and G_v is utilized to convert diffraction limited linear polarization into an optical spot with circular or elliptical polarization beyond the diffraction limit. A parameter that plays a key role in this conversion is the polarization angle α_{pol} of the incident linearly polarized radiation, which is used to adjust the relative amplitude of the horizontal and vertical field components.

The effect of G_h-G_v on $\Delta\phi$ and E_y/E_x is illustrated in Fig. 4. The rectangular aperture is illuminated with a linearly polarized incident field with $\alpha_{\text{pol}}=45^\circ$. In Fig. 4, $\Delta\phi$ and E_y/E_x are plotted as a function of G_v at the point $x=0$, $y=0$, and $z=20$ nm. In Fig. 4(a) a phase difference,

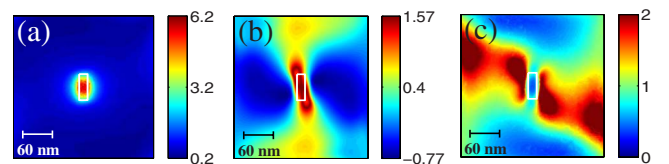


FIG. 5. (Color online) (a) $|E|^2$, (b) $|\Delta\phi|$, and (c) $|E_y|/|E_x|$ for $\phi_{\text{pol}}=45^\circ$, $G_h=20$ nm, and $G_v=60.5$ nm.

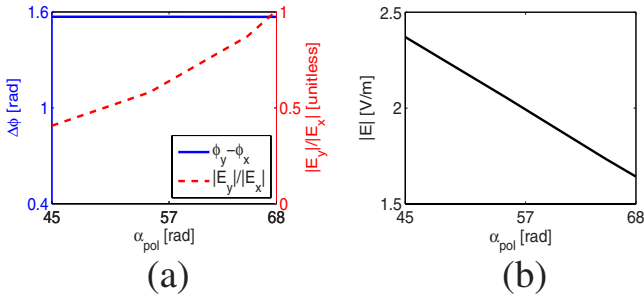


FIG. 6. (Color online) Effect of various α_{pol} values on (a) $|\Delta\phi|$ and $|E_y|/|E_x|$ and (b) $|E|^2$ for $G_h=20$ nm, $G_v=60.5$ nm, and $T=20$ nm.

$\Delta\phi \neq 0$, is obtained by creating an asymmetry between G_h and G_v . At $G_v=60.5$ nm we obtain $E=2.37$ V/m, $\Delta\phi=1.57$ radians, and $E_y/E_x=0.4$, which indicates an elliptically polarized optical spot. As G_v decreases to 20 nm, $\Delta\phi$ decreases to 0 rad, since the aperture becomes symmetric and the phase difference due to G_h-G_v vanishes, resulting in a linearly polarized beam. The results suggest that an elliptically polarized near-field radiation is obtained for G_v values between 20 and 60.5 nm. When G_v is exactly 20 nm, the localized radiation becomes linearly polarized. In Fig. 5, $|E|^2$, $\Delta\phi$, and E_y/E_x are plotted on the $z=20$ cut-plane for $G_h=20$ nm and $G_v=60.5$ nm. As shown in Fig. 5(b), the $\Delta\phi$ value of 1.57 rad is achieved at $G_v=60.5$ nm.

To achieve a circularly polarized optical spot, a $\Delta\phi$ value of 1.57 rad is not sufficient. In addition, E_y/E_x should be unity. To reach circular polarization, E_y/E_x needs to be further increased. As shown in Fig. 6, E_y/E_x is increased from 0.4 to 1 by changing α_{pol} of the incident linear radiation from 45° to 68° . As shown in Fig. 6, as α_{pol} is increased to 68° , $\Delta\phi$ keeps constant around 1.57 rad, while E decreases to 1.64 V/m. Localized near-field radiation is achieved as shown in Fig. 7(a). Localization of $\Delta\phi$ and E_y/E_x is shown in Figs. 7(b) and 7(c). Around the optical spot, $\Delta\phi$ and E_y/E_x are 1.57 rad and 1, respectively. Therefore, a left-handed circularly polarized optical spot is obtained in Fig. 7.

LSP play an important role in obtaining intense optical spots and converting linearly polarized diffraction limited radiation into a circularly polarized spot beyond the diffraction limit. The desired phase difference and amplitude ratio in Fig. 7 is a result of (i) the significantly shorter wavelength of the LSP as compared to the wavelength of the incident pho-

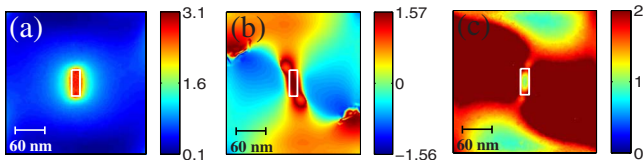


FIG. 7. (Color online) (a) $|E|^2$, (b) $|\Delta\phi|$, and (c) $|E_y|/|E_x|$ for $\alpha_{\text{pol}}=68^\circ$, $G_h=20$ nm, and $G_v=60.5$ nm.

tons and (ii) an asymmetric aperture. By creating an asymmetry in the aperture shape, an optical path difference is created between LSP in the horizontal and vertical directions, which is tuned to obtain a 90° phase difference. The amplitude ratio is tuned using α_{pol} in Fig. 7.

In summary, circularly and elliptically polarized optical spots beyond the diffraction limit are achieved via subwavelength apertures. It was demonstrated that a square nanoaperture can mediate diffraction limited circularly or elliptically polarized radiation into a circularly or elliptically polarized optical spot well beyond the diffraction limit, respectively. It was also shown that a phase difference can be obtained between field components by utilizing a rectangular nanoaperture. Linearly polarized diffraction limited radiation was converted into a circularly or elliptically polarized optical spot well-beyond the diffraction limit using a rectangular aperture.

This work is supported by TUBITAK (Grant No. 108T482), European Community Marie Curie International Reintegration Grant (Grant No. MIRG-CT-2007-203690), and partially by the Turkish Academy of Sciences.

- ¹L. Novotny and B. Hecht, *Principles of Nano-Optics* (Cambridge University Press, New York, 2006).
- ²H. A. Bethe, *Phys. Rev.* **66**, 163 (1944).
- ³Y. Leviatan, *J. Appl. Phys.* **60**, 1577 (1986).
- ⁴T. W. Ebbesen, H. J. Lezec, H. F. Ghaemi, T. Thio, and P. A. Wolff, *Nature (London)* **391**, 667 (1998).
- ⁵H. J. Lezec, A. Degiron, E. Devaux, R. A. Linke, L. Martin-Moreno, F. J. Garcia-Vidal, and T. W. Ebbesen, *Science* **297**, 820 (2002).
- ⁶F. J. Garcia de Abajo, *Opt. Express* **10**, 1475 (2002).
- ⁷C. Genet and T. W. Ebbesen, *Nature (London)* **445**, 39 (2007).
- ⁸K. Aydin, A. O. Cakmak, L. Sahin, Z. Li, F. Bilotti, L. Vegni, and E. Ozbay, *Phys. Rev. Lett.* **102**, 013904 (2009).
- ⁹J. G. Rivas, C. Schotsch, P. Haring Bolivar, and H. Kurz, *Phys. Rev. B* **68**, 201306 (2003).
- ¹⁰C. D. Stanciu, F. Hansteen, A. V. Kimel, A. Kirilyuk, A. Tsukamoto, and A. Itoh, *Phys. Rev. Lett.* **99**, 047601 (2007).
- ¹¹Y. Ohdaira, T. Inoue, H. Hori, and K. Kitahara, *Opt. Express* **16**, 2915 (2008).
- ¹²T. Shegai, Z. Li, T. Dadoosh, Z. Zhang, H. Xu, and G. Haran, *Proc. Natl. Acad. Sci. U.S.A.* **105**, 16448 (2008).
- ¹³P. Biagioni, J. S. Huang, L. Duò, M. Finazzi, and B. Hecht, *Phys. Rev. Lett.* **102**, 256801 (2009).
- ¹⁴E. Ogut, G. Kiziltas, and K. Sendur, *Appl. Phys. B* **99**, 67 (2010).
- ¹⁵P. Biagioni, M. Savoini, J. S. Huang, L. Duò, M. Finazzi, and B. Hecht, *Phys. Rev. B* **80**, 153409 (2009).
- ¹⁶R. Kullock, *Opt. Express* **16**, 21671 (2008).
- ¹⁷A. Drezet, C. Genet, and T. Ebbesen, *Phys. Rev. Lett.* **101**, 043902 (2008).
- ¹⁸T. Li, H. Liu, S. M. Wang, X. G. Yin, F. M. Wang, S. N. Zhu, and X. Zhang, *Appl. Phys. Lett.* **93**, 021110 (2008).
- ¹⁹K. Şendur, W. Challener, and C. Peng, *J. Appl. Phys.* **96**, 2743 (2004).
- ²⁰K. Şendur, C. Peng, and W. Challener, *Phys. Rev. Lett.* **94**, 043901 (2005).
- ²¹E. D. Palik, *Handbook of Optical Constants of Solids* (Academic, New York, 1998).